Original article

Median nerve stiffness with three movement sequences of the upper limb neurodynamic test 1: An ultrasound shear-wave elastography study

Gianluca Ciuffreda [a], Elena Estébanez-de-Miguel [a], Isabel Albarova-Corral [a], Miguel Malo-Urriés [a], Michael Shacklock [b], Alberto Montaner-Cuello [a], Elena Bueno-Gracia [a,*]

[a] Department of Physiatry and Nursing, Faculty of Health Sciences, University of Zaragoza, Zaragoza, Spain
[b] Neurodynamic Solution, Adelaide, Australia

ABSTRACT

Background: During the Upper Limb Neurodynamic Test 1 (ULNT1) joint movement order can be varied to improve its diagnostic accuracy. However, nerve behavior with neurodynamic sequences still requires in vivo research.
Objective: To quantify differences in median nerve (MN) stiffness measuring shear-wave velocity (SWV) with ultrasound elastography during three sequences of the ULNT1.
Design: Cross-sectional study.
Methods: MN SWV was measured in 35 asymptomatic subjects at the wrist and elbow at the initial and final position (P1) of the standard (ULNT1-STD), proximal-to-distal (ULNT1-PROX) and distal-to-proximal (ULNT1-DIST) sequences of the ULNT1.
Results: Significantly different increases at P1 in nerve stiffness occurred between sequences and locations (p < 0.001). At the wrist, the ULNT1-PROX produced the smallest increase (44.32% ± 44.06, SWV: 4.49 ± 0.95 m/s), the ULNT1-STD produced a larger increase (82.13% ± 45.36, SWV: 5.67 ± 0.79 m/s, p < 0.001) and the ULNT1-DIST produced the largest (92.90% ± 55.37, SWV: 5.97 ± 0.79 m/s, p < 0.001). Differences between the ULNT1-DIST and ULNT1-STD did not reach significance.
At the elbow, the ULNT1-PROX showed a 119.92% ± 53.51 increase (SWV: 4.08 ± 0.84 m/s), the ULNT1-DIST a 134.84% ± 53.83 (SWV: 4.34 ± 0.77 m/s), and the ULNT1-STD a 113.30% ± 59.28 (SWV: 3.98 ± 1.04 m/s). No significant differences were found among the sequences.
Conclusion: The ULNT1-STD and ULNT1-DIST showed greater increases at MN stiffness at the wrist compared to the ULNT1-PROX. This supports a basis for future investigation of the mechanisms of neurodynamic testing in which emphasizing anatomical locations for improving diagnostic efficacy might be applied.

1. Introduction

The upper limb neurodynamic test 1 (ULNT1) is used for the clinical evaluation of conditions such as carpal tunnel syndrome and cervical radiculopathy (Bueno-Gracia et al., 2016; Hall and Elvey, 1999; Nee et al., 2012; Schmid et al., 2009; Wainner et al., 2003). The test uses a series of joint movements to elongate the nerve bed and apply tension along the median nerve tract, brachial plexus and lower cervical nerve roots (Bueno-Gracia et al., 2016; Hall and Elvey, 1999; Nee et al., 2012; Schmid et al., 2009; Wainner et al., 2003; Shacklock, 2005a, 2005b).

Test movements can be varied to produce changes in nerve behavior (Hall and Elvey, 1999; Shacklock, 2005a, 2005b; Butler, 1991; Nee et al., 2010; Boyd et al., 2013), such as with the sequence (order) and range of joint movements and distance from the clinical problem (Shacklock, 1989). For instance, initiating movement at the wrist can improve diagnostic efficacy in carpal tunnel syndrome in the form of increased specificity (e.g. 95.7%) compared to the standard sequence of the ULNT1 (Bueno-Gracia et al., 2016, 2024). Whether sequencing affects nerve behavior has been studied in embalmed cadavers in which initiating the test at the elbow (flexion) for the ulnar neurodynamic test

increases strain by 18% over sequences that start at the shoulder or wrist (Tsai, 1995). How this occurs remains in question because, when the ULNT1 is performed in fresh cadavers to the same range for different sequences, the nerve strain at the wrist at the end position is similar for all sequences. This suggested that strain may not be as relevant as originally thought and instead duration at the end position might be more important (Nee et al., 2010).

The above results were obtained in cadavers, but when the conscious subject limits the range of each joint movement by expressing the onset or maximum tolerance of responses (e.g. stretch, pain or paraesthesiae), the range of each joint with different sequences changes and nerve behavior is likely to differ. For instance, clinically, when wrist extension is moved first, a large range occurs and the next movements (elbow extension, shoulder abduction) are more restrained than occurs with a standard ULNT1 sequence. This reverses when shoulder abduction occurs first, whereby wrist extension becomes more restrained. Considering that nerves do not behave uniformly along their course and respond to variations in loading (Shacklock, 2005b; Boyd et al., 2013; Rugel et al., 2020), the ULNT1 may be used as a model to investigate nerve behavior at response onset at certain locations with various sequences of movement (Shacklock, 2005a; Nee et al., 2010; Boyd et al., 2013; Greening and Dilley, 2017). This would fill a gap in knowledge of nerve behavior with neurodynamic sequencing.

Shear-wave elastography (SWE) is an ultrasound-integrated technique that allows the in vivo assessment of tissue mechanical properties (stiffness) (Youk et al., 2013; Yoon et al., 2014; Lee et al., 2013; Zakrzewski et al., 2019; Lin et al., 2019; Taljanovic et al., 2017) suitable for the evaluation of nerve behavior in response to joint movement (Rugel et al., 2020; Ciuffreda et al., 2024; Andrade et al., 2016, 2022; Lee et al., 2019). It reflects nerve stiffness by measuring the velocity of a shear wave that is produced in tissue after emission of an acoustic pulse (greater velocity, stiffer nerve) (Taljanovic et al., 2017; Nightingale, 2011). In addition to being valid and reliable in diagnosis of carpal tunnel syndrome and other peripheral neuropathies (Zakrzewski et al., 2019; Lin et al., 2019; Taljanovic et al., 2017; Wee and Simon, 2019), SWE can be used to study nerve stiffness during variations in the ULNT1 (Greening and Dilley, 2017; Ciuffreda et al., 2024; Lin et al., 2022).

The aim of this study was therefore to compare MN behavior (stiffness) at the wrist and elbow with three sequences of the ULNT1 by quantifying nerve shear wave velocity (SWV). As peripheral nerves can exhibit regional variations in their anatomy and mechanical properties (Andrade et al., 2022), investigating the response of different nerve segments to different loading patterns based on the order of joint movement will provide a better understanding of nerve biomechanics during neurodynamic testing. From a clinical perspective, this may help optimize the ULNT1 application for different pathological situations and potentially increase its diagnostic capacity to detect localized alterations in a specific nerve segment such as carpal tunnel syndrome.

We hypothesized that MN SWV would be greater at the wrist if a distal-to-proximal sequence (ULNT1-DIST) was performed, compared to the standard sequence (ULNT1-STD) (Shacklock, 2005b) or a proximal-to-distal sequence (ULNT1-PROX), in which wrist extension is performed later.

2. Materials and methods

2.1. Study design

A cross-sectional study was carried out. The local Institutional Ethical Committee (CEICA, reference: C.I. PI22/525) approved the study and all procedures conformed to the Declaration of Helsinki (last modified in 2013) (World Medical Association declaration of Helsinki, 2013). Informed written consent was obtained from all participants prior to the data collection. This study was carried out according to the STROBE guidelines (Cuschieri, 2019).

2.2. Sample

A sample of thirty-five healthy volunteers was recruited from February to May 2023 through advertisements on social media. Participants must meet the following inclusion criteria: aged between 18 and 65; having a full passive range of motion in all joints involved in the ULNT1 and the structural differentiation movements; having comprehensive and communicative capacity. Exclusion criteria were: reported pain, altered sensitivity, paresthesia or dysesthesia, weakness at the level of the spine or upper limb in the previous 12 months; any type of injury to the thoracic or cervical spine or upper limb in the previous 12 months; any type of autoimmune disease; diabetes or thyroid disorders; central nervous system disorders. In order to show a similar nerve biomechanics, participants must present symptoms in a range between 120° and 170° of elbow extension (Lohkamp and Small, 2011) in the ULNT1-STD (Shacklock, 2005b). Additionally, MN SWE measurements were performed only when a ULNT1 sequence showed a positive structural differentiation. All participants provided informed and written consent. After receiving the written consent to participate, the following base-line demographic details were recorded from all participants: sex, age, height, weight, and body mass index.

A power analysis with the data obtained from the thirty-five participants initially recruited was performed using G*Power 3.1 (Faul et al., 2007) (Faul et al., 2007). The power analysis was calculated for the interaction between upper limb positions and MN locations obtained with a two-way repeated measures ANOVA. The "SWV" and the "increase in SWV from the starting position" were used as dependent variables. The partial η^2 value used for the calculation was 0.208, which represented the lowest value among the interactions above mentioned. With an α level set at 0.05 and a sample size of thirty-five participants, the statistical power obtained was 1.00. Therefore, we concluded that no additional subjects needed to be recruited.

2.3. Ultrasound procedures and shear-wave elastography

MN SWE was performed using a LOGIQ P9 ultrasound system (GE healthcare medical system, USA) with high-frequency linear transducer L3-12 (12-MHz). During the SWE scans, the spatial and temporal filters predefined in the system were used. Specifically, the system's settings for musculoskeletal applications "Nerve" were applied, which include a spatial filter setting of 5 and a temporal filter setting of 4. The spatial resolution of the SWE images was set to 1 mm. In each subject, the right median nerve was imaged at two locations: 1) immediately proximal to the wrist crease at the quadratus pronator level (Moran et al., 2020); 2) immediately proximal to the elbow (Greening and Dilley, 2017). MN was first identified in the transverse plane by its honeycomb-like structure and by following the nerve path along the upper extremity with the ultrasound probe. The transverse imaging plane of the nerve was obtained by B-mode. The transducer was then rotated 90° into the longitudinal plane and aligned with the direction of the nerve fibers to perform SWE measurements. Shear wave elastography was applied in dual mode (elastogram displayed alongside grey-scale imaging) within a 2.0×2.0 cm box including MN with its surrounding tissues and avoiding any bony regions. The elastogram displayed tissue shear-wave velocity (SWV) on a color scale set from 0 (dark blue) to 10 m/s (red). Shear wave elastography values (m/s) were obtained automatically for each image from a manually traced region of interest (ROI) including the entire area of the nerve contained in the elastography box (Fig. 1). The average SWV from three measurements was used for further analysis.

Additionally, MN thickness (mm) and angle (°) were measured at both locations. MN thickness was measured by manually tracing a straight line within the epineurium boundaries in the area corresponding to the mid-portion of the nerve included in the elastography box. Nerve angle was determined by calculating the degrees between the longitudinal axis of the nerve segment comprised in the elastography box and a horizontal line across the ultrasound image. All ultrasound

a)

b)
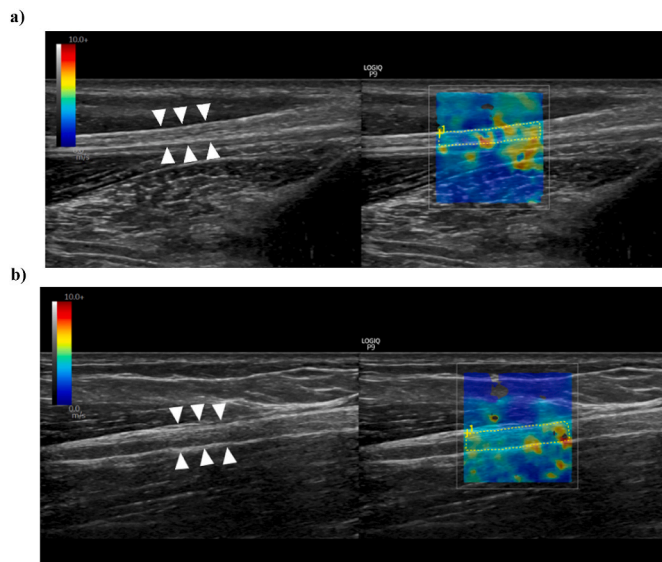
Fig. 1. Example of MN SWE measurement at the pronator quadratus level (a) and immediately proximal to the elbow (b).

data were collected by the same examiner (GC) using minimal transducer pressure and the necessary amount of coupling ultrasound gel. Room temperature was maintained at 21 °C.

White head arrows: median nerve. The discontinuous yellow lines indicate the evaluated Region of Interest (ROI), obtaining the Shear-Wave Velocity (SWV) expressed in meters per second (m/s). B-mode grey scale: from black (anechoic) to white (hyperechoic). SWV color scale: from dark blue (0 m/s) to red (10 m/s).

2.4. Upper limb neurodynamic test 1 sequences

Each participant was imaged in the initial position (P0) and at the final position (P1) of the ULNT1-STD, ULNT1-PROX and ULNT1-DIST with a 3-min rest between each test (Vanti et al., 2010). The order of the ULNT1 sequence was determined randomly.

In the initial position (P0), participants were supine, with the cervical spine in neutral position and the face in the horizontal plane, the shoulder girdle in a neutral position, 30° of glenohumeral abduction in neutral rotation, 90° of elbow flexion, forearm, wrist and fingers in a neutral position. Then, one examiner (MMU) performed the randomized sequence of the ULNT1 until the onset of any sensory response, including but not limited to tension, pain, tingling, pins and needles or

Table 1
ULNT1 joint movements and order for each neurodynamic sequence.

ULNT1-STD (Shacklock, 2005b)
1) Shoulder abduction from 90° to 110°
2) Shoulder external rotation to the frontal plane
3) Forearm supination
4) Wrist and finger extension
5) Elbow extension
ULNT1-PROX
1) Cervical contralateral lateral flexion
2) Shoulder abduction from 90° to 110°
3) Shoulder external rotation to the frontal plane
4) Elbow extension
5) Forearm supination
6) Wrist and finger extension
ULNT1-DIST
1) Wrist and finger extension
2) Forearm supination
3) Elbow extension
4) Shoulder external rotation to the frontal plane
5) Shoulder abduction

numbness. Participants were previously instructed to verbalize the word "stop" the moment they started to feel the any sensory response in the tested limb. During each test, the scapula was manually stabilized by pressing the knuckles firmly against the bed above the participant's shoulder to prevent elevation while performing limb or neck movements (Bueno-Gracia et al., 2016; Shacklock, 2005b; Vanti et al., 2010, 2011). Special attention was taken to ensure that no scapular depression was applied in any sequence. The movements of each ULTN1 sequence and their respective order are described in Table 1.

Structural differentiation was performed in all the three sequences of the ULNT1 to verify the neural origin of symptoms (Bueno-Gracia et al., 2016, 2019, 2020a, 2020b, 2021; Nee et al., 2012; Shacklock, 2005b; Butler, 1991; Lohkamp and Small, 2011; Elvey, 1997; Herrington et al., 2008; Pesonen et al., 2021). If participants reported distal responses, structural differentiation was performed with movement of the neck or shoulder girdle. While for the proximal localization of responses, structural differentiation consisted of movement of the wrist.

At the end of each ULNT1, range of motion (ROM) of the last joint moved was recorded for elbow extension, shoulder abduction and wrist dorsiflexion. ROM measurements were performed at the end of the test by a third examiner (IAC) using a standard 360° two-arm goniometer. For the elbow extension angle, the axis of the goniometer was placed on the medial epicondyle of the humerus, with the stationary arm of the goniometer pointing in the direction of the acromion and the moving arm aligned with the ulnar styloid (Lohkamp and Small, 2011; Rothstein et al., 1983). The glenohumeral abduction angle was recorded by placing the axis of the goniometer at the level of the acromion, with the stationary arm parallel to the sternum and the moving arm aligned with the medial epicondyle of the humerus (Martínez et al., 2014; Riddle et al.). The wrist dorsiflexion angle was measured from the ulnar side, placing the axis of the goniometer at the level of the lunate bone, aligning the stationary arm with the olecranon and the moving arm with the third metacarpal bone (LaStayo and Wheeler Donna, 1995; Carter et al., 2009).

2.5. Reliability

The reliability of MN SWE was investigated in 10 upper limbs from five participants (age: 39.8 ± 5.8 years; 2 males and 3 females). Intra-rater reliability was assessed at the wrist and elbow level performing two assessments in each location with the participant in supine with the cervical spine in neutral and the upper extremity relaxed in 30° of abduction. The mean SWV from two elastographies were used for the analysis. Reliability was calculated with a two-way mixed effect intraclass correlation coefficient (ICC) "absolute agreement" (Koo and Li, 2016). The standard error of measurement (SEM) and the minimal detectable change (MDC) were calculated as follows: SEM = standard deviation x $\sqrt{(1-ICC)}$; MDC = SEM x 1.96 x $\sqrt{2}$.

2.6. Statistical analysis

Statistical analysis was performed using SPSS 29.0 software (SPSS Inc., Chicago, IL, USA). The Shapiro-Wilk test was used to check the normal distribution of data. The mean ± standard deviation (SD) was used to express quantitative data, unless otherwise stated. For all SWV analysis, the average value obtained from three elastographies (three images) was used. For the analysis of the increase in SWV, the percentage of change of SWV values at P1 with respect to the initial measurement at P0 was used. A two-way repeated measures ANOVA was conducted to compare MN SWV, thickness and angle, at both the wrist and elbow in each limb position (P0 and P1 of all ULNT1 sequences). Additionally, a two-way repeated measures ANOVA was also performed to compare the percentage of change in SWV from P0 at the end of each ULNT1 sequence in both MN locations. In all ANOVA analyses, the assumption of sphericity was evaluated using the Mauchly test. If this

assumption was violated, the degrees of freedom were adjusted using Greenhouse-Geisser correction. Post hoc comparisons were accounted for by using Bonferroni corrections. Correlations between SWV, nerve thickness and angle were analysed using Spearman's correlation coefficient (r_s). α level was set at 0.05.

3. Results

Thirty-five healthy participants (20 females, 15 males) were enrolled in the study (age: 34.37 ± 11.06 years, height: 1.74 ± 0.10 m, weight: 69.27 ± 11.63 kg, body mass index: 22.82 ± 2.89, dominant side: 33 right and 2 left). No subjects were excluded and SWE measurements were performed for all ULNT1 sequences.

The results of MN SWE reliability study are shown in Table 2.

3.1. Median nerve shear-wave velocity

MN SWV data are summarized in Fig. 2.

At P0 mean SWV was 3.29 ± 0.88 m/s at the wrist and 1.90 ± 0.37 m/s at the elbow ($p < 0.001$). All ULNT1 sequences produced an increase in SWV respect to P0 in both MN locations ($p < 0.001$).

The ULNT1-STD increased SWV by 82.13% ± 45.36 at the wrist and by 113.30% ± 59.28 at the elbow (mean difference: 31.17%; $p = 0.019$), with values at P1 of 5.67 ± 0.79 m/s and 3.98 ± 1.04 m/s respectively (mean difference: 1.692 m/s; $p < 0.001$).

The ULNT1-PROX lead to a smaller difference in MN SWV at P1 between the wrist and the elbow (4.49 ± 0.95 m/s; 4.08 ± 0.84 m/s; mean difference 0.412; $p = 0.034$), however SWV in the elbow showed a greater increase from P0 than in the wrist (119.92% ± 53.51; 44.32% ± 44.06; mean difference: 75.59%; $p < 0.001$).

Median nerve SWV at P1 in the ULNT1-DIST was 5.97 ± 0.79 m/s in the wrist and 4.34 ± 0.77 m/s in the elbow (mean difference: 1.624 m/s; $p < 0.001$), the increase from P0 was respectively 92.90% ± 55.37 and 134.84% ± 53.83 (mean difference: 41.95%; $p = 0.004$).

Two-way repeated measures ANOVA revealed a significant interaction between position and MN location for the SWV ($p < 0.001$), and between ULNT1 sequence and MN location for the percentage of increase in SWV from P0 ($p < 0.001$).

Post hoc analysis with multiple comparisons showed statistically significant differences in MN SWV at the wrist between the ULNT1-STD and the ULNT1-PROX (mean difference: 1.180 m/s; $p < 0.001$), the ULNT1-PROX and the ULNT1-DIST (mean difference: 1.476 m/s; $p < 0.001$) but not the ULNT1-STD and the ULNT1-DIST ($p = 0.385$). At the elbow SWV at P1 was similar in each ULNT1 sequence ($p > 0.05$).

In terms of percentage change from P0, the ULNT1-PROX was the sequence that produced significantly less increase in SWV at the wrist from the initial position ($p < 0.001$). In the same location, the ULNT1-DIST showed the largest change from P0, however it was significant only compared to the ULNT1- PROX ($p < 0.001$). At the elbow all ULNT1 sequences produced a similar increase of MN SWV ($p > 0.05$).
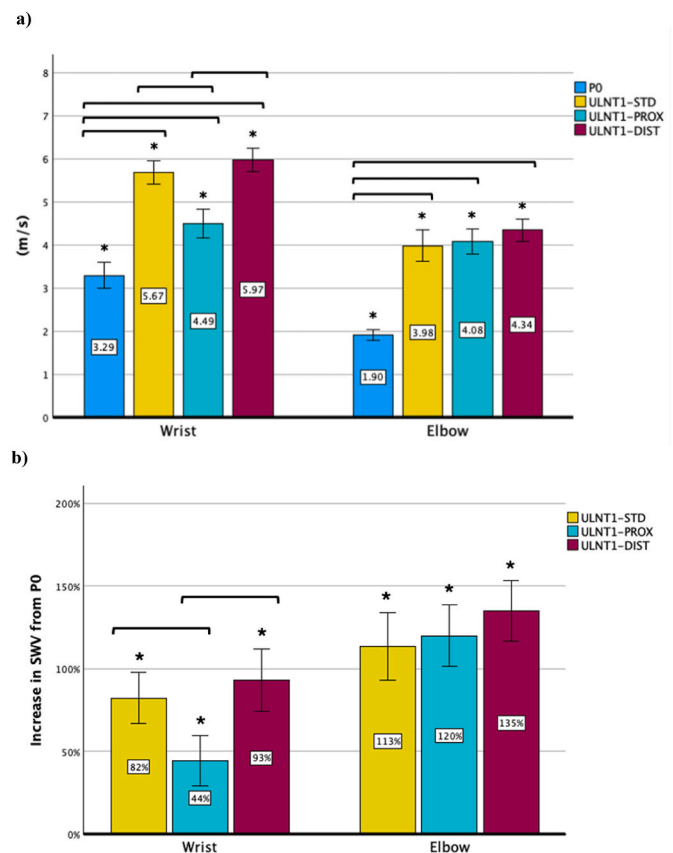
Horizontal Bars = statistically significant difference comparing two positions at the same location. * = statistically significant difference between the wrist and the elbow in the same position. Error Bars = 95% Confidence Interval.

Fig. 2. Median nerve SWV (a) at P0 and at the end point of each ULNT1 sequence and (b) SWV increase from P0.

3.2. ULNT1 end-stage and range of motion

The ULNT1 end-stage and the ROM of the last joint moved are shown in Table 3. In the ULNT1-STD, all participants reported responses during elbow extension, with an average ROM of 146.4° ± 15.04. In the ULNT1-PROX most of the subjects presented responses during elbow extension (n = 32; mean ROM 154.91° ± 14.53), while three subjects during wrist extension (mean ROM 39.33° ± 12.22). In the ULNT1-DIST, all subjects reported the onset of responses during glenohumeral abduction, with a mean ROM of 47.57 ± 19.39.

3.3. Median nerve thickness and angle

Mean nerve thickness and angle values for each location and position are reported in Table 3.

MN was thicker at the elbow than at the wrist (mean difference: 0.661 mm; $p < 0.001$), however, no significant interaction between position and location was found for nerve thickness ($p = 0.303$).

Two-way repeated measures ANOVA revealed a significant interaction between position and location for nerve angle ($p < 0.001$). Post-hoc analysis showed statistically significant differences in MN angle at the elbow at P1 of ULNT1-DIST compared to ULNT1-STD (mean difference: 2.05°, $p = 0.003$) and compared to P0 (mean difference: 2.54°, $p = 0.003$). No other significant differences were found for nerve angle among the two MN locations and limb positions.

A weak negative correlation was found between MN thickness and SWV (r_s: 0.185, $p = 0.002$), whereas nerve angle showed no significant correlation with SWV (r_s: 0.002, $p = 0.969$).

Table 2
Intra-rater reliability of MN SWE assessment.

	ICC	SEM	MDC
Wrist	0.927	0.101	0.279
Elbow	0.940	0.109	0.301

ICC = intraclass correlation coefficient. SEM = standard error of measurement. MDC = minimal detectable change.

4. Discussion

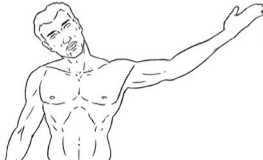The results of the present study showed that the mechanical behavior of the median nerve at the wrist and elbow, measured with SWV, differed with three sequences of movements of the ULNT1. However, these differences were not significant for all sequences. At the wrist, MN SWV was significantly lower in the ULNT1-PROX compared to the other two sequences. The ULNT1-DIST produced higher SWV values, however it was only statistically significant compared to the ULNT1-PROX. It has been reported that wrist extension significantly increases SWV in the distal portion of the MN in both elbow flexion and extension positions (Greening and Dilley, 2017; Ciuffreda et al., 2024). This behavior could possibly explain the non-significant difference in MN SWV between the ULNT1-STD and the ULNT1-DIST as well as the lower SWV values reported for the ULNT1-PROX, where wrist extension could not be completed in most of the subjects before response onset. The pattern of influences of sequence on the nerve was different at the elbow, where all ULNT1 sequences produced a similar increase in SWV.

The results of the present study seem to support partially the idea of neurodynamic sequencing theorized by previous authors (Shacklock, 2005a, 2005b; Butler, 1991). Movements that are supposed to place the nerve under tension can lead to an increase in its SWV (Rugel et al., 2020; Greening and Dilley, 2017; Ciuffreda et al., 2024). Therefore, the differences in MN SWV observed between the three ULNT1 sequences performed may implicate that a specific neural segment is subjected to loading patterns with the order of joint movement during a neurodynamic test. The effects of neurodynamic sequencing have been tested in cadaveric studies, which reported similar levels of strain and excursion for MN and sciatic/tibial nerve at the end of a neurodynamic test regardless of the order of joint movement. The joint movements were similar with all sequences in those studies, but our study produced different final joint positions which might have influenced the end stiffness in the nerve.

In a clinical context, a neurodynamic test is usually concluded with the appearance of symptoms (Nee et al., 2012; Schmid et al., 2009; Shacklock, 2005b; Butler, 1991), which can result in variations in joints ranges depending on how the test is carried out. When performing a neurodynamic test sequence, the neural load progressively increases as joint movements are added to the test, consequently, the first joint range of movement is often large because it is initially unconstrained, while if the same movement occurs at the end of a test, it frequently does not reach its full range because of the onset of symptoms (Coppieters et al.,

Table 3

Starting position and ULNT1 end-stages with ROM of the last joint moved. At each position mean median nerve thickness and angle are reported and an example of nerve shear-wave elastography is shown.

P0

N= 35

Wrist
Thickness (mm): 2.22 ± 0.54.
Angle (°): 3.99 ± 2.77.

Elbow
Thickness (mm): 3.04 ± 0.63.
Angle (°): 5.22 ± 3.55.

ULNT1-STD

N= 35

End-stage: elbow extension.
ROM (°): 146.4 ± 15.04.

Wrist
Thickness (mm): 2.45 ± 0.33.
Angle (°): 5.34 ± 2.29.

Elbow
Thickness (mm): 3.02 ± 0.52.
Angle (°): 4.72 ± 2.05.

ULNT1-PROX

N= 32

End-stage: elbow extension.
ROM (°): 154.91 ± 14.53.

Wrist
Thickness (mm): 2.41 ± 0.28.
Angle (°): 4.84 ± 1.71.

Elbow
Thickness (mm): 3.09 ± 0.41.
Angle (°): 4.03 ± 2.41.

N= 3
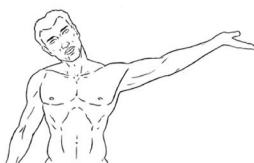
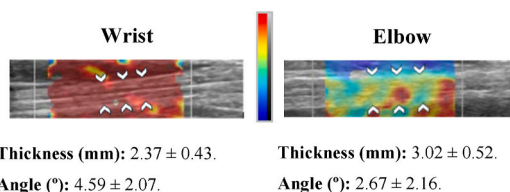**End-stage:** wrist extension.

ROM (°): 39.33 ± 12.22.

ULNT1-DIST

N= 35

Wrist

Thickness (mm): 2.37 ± 0.43.
Angle (°): 4.59 ± 2.07.

Elbow

Thickness (mm): 3.02 ± 0.52.
Angle (°): 2.67 ± 2.16.

End-stage: shoulder abduction.

ROM (°): 47.96 ± 15.96.

ROM = range of motion. White head arrows: median nerve. SWV color scale: from dark blue (0 m/s) to red (10 m/s).

2002a). Therefore, when different neurodynamic sequences are applied, changes in nerve behavior may occur at the end of a test due to the impact of different joint motion ranges. These considerations might explain the difference between our results and previous research (Nee et al., 2010; Boyd et al., 2013).

Our findings suggest that neurodynamic sequencing may be an option for clinicians to increase the mechanical load in the nerve portion located in the proximity of the first joints moved during the ULNT1. Moving joints through different ranges may also expose a nominated neural segment to a greater amount of external pressure (Noah Weiss et al., 1995) and a higher tension for a longer time (Nee et al., 2010; Boyd et al., 2013). These mechanisms could also contribute to justify the clinical application of neurodynamic sequences, and might reflect the higher values for carpal tunnel syndrome diagnosis reported by Bueno et al. (Bueno-Gracia et al., 2024) in comparison to previous research (Bueno-Gracia et al., 2016; Vanti et al., 2011, 2012; Trillos et al., 2018; Wainner et al., 2005). However, since different ULNT1 sequences were not directly compared, further investigations are required to fully understand the impact of using different neurodynamic sequences on the diagnostic efficacy of the test.

Moreover, the ULNT1 is widely used in clinical practice in the assessment of a variety of neural conditions with competitive diagnosis and different anatomical source, i.e. cervical radiculopathy and carpal tunnel syndrome (Bueno-Gracia et al., 2016; Hall and Elvey, 1999; Nee et al., 2012; Schmid et al., 2009; Wainner et al., 2003, 2005; Vanti et al., 2011, 2012; Trillos et al., 2018; Apelby-Albrecht et al., 2013). According to our findings, the ULNT1-PROX sequence applies less mechanical load to the MN at the wrist compared to other sequences, while maintaining a similar load more proximally. By using neurodynamic sequencing, clinicians may direct neural stress toward targeted areas suspected of involvement and, at the same time, perform the test with reduced load on more remote nerve segments. The ability to modify neural load distribution during the ULNT1 could play an interesting role in differential diagnosis, when symptoms present similar characteristics but have different regional origin. For instance, the ULNT1-PROX sequence may be more prone to reproduce symptoms associated with cervical radiculopathy, while being less likely to provoke symptoms related to carpal tunnel syndrome. Nevertheless, further studies are needed to investigate nerve behavior with neurodynamic sequencing in more proximal regions (e.g. cervical nerve roots, brachial plexus, etc.), as well as its potential additional value in differential diagnosis.

Standardized sequences during neurodynamic test have been generally recommended by previous authors in order to enhance reproducibility (Shacklock, 2005b; Butler, 1991). Despite the slight variations across studies in how the test is performed, high intra-rater reliability values have been reported for the ULNT1 whether the test is performed in laboratory (i.e. using stabilizing devices) or clinical environment (Vanti et al., 2010; Coppieters et al., 2002b; Talebi et al., 2012; Oliver and Rushton, 2011; Riley et al., 2020; Legakis and Boyd, 2012). Considering this, we decided not to employ any stabilizing devices to support the upper limb, which allowed to perform the ULNT1 sequences more similarly to a clinical setting. Also, some authors have included scapular depression in their testing protocols (Apelby-Albrecht et al., 2013; Talebi et al., 2012; Legakis and Boyd, 2012). To maintain consistency with the standard sequence as described by Shacklock (2005) (Shacklock, 2005b) and simplify comparisons across tests, we did not incorporate scapular depression in any of the sequences. Despite this, including scapular depression in certain sequences could be an option to enhance regional differences in neural load distribution. For instance, adding scapular depression in the ULNT1-PROX sequence, could reduce the participation of distal joints (Legakis and Boyd, 2012) and potentially result in less stiffness in the distal portion of MN compared to other sequences.

Furthermore, some additional aspects must be considered regarding nerve SWE.

In an elastic, homogeneous, and isotropic medium, the shear modulus (μ) can be calculated with the equation $\mu = \rho c^2$, where ρ is the density (assuming ρ = 1000 kg/m^3), and c is the shear wave speed.

Young's modulus (E) can be approximated as three times the shear modulus: E = 3μ (Bercoff et al., 2004). Peripheral nerves are relatively thin, layered structures with anisotropic characteristics. Consequently, the relationship between SWV and the Young's modulus, which does not account for anisotropic tissues, in nerves can only be considered an estimate (Shiina et al., 2015). When a tissue presents a stiff nature and finite thickness relative to the shear wavelength, it may be subjected to guided propagation of shear waves (Brum et al., 2014), potentially leading to biases in SWV measurements. In this study, the MN was 0.661 mm thicker at the elbow compared to the wrist. Nevertheless, nerve thickness did not vary among the different limb positions and showed a weak negative correlation with SWV, which contrasts with the expected guided wave propagation behavior (Andrade et al., 2022; Mo et al., 2016). This suggests that SWV measurements are unlikely to be substantially biased by guided waves in the current study. Additionally, as anisotropic tissues, the orientation of the nerve relative to the ultrasound probe can also affect SWV measurements. To minimize this effect, the ultrasound probe was positioned as perpendicular to the nerve as possible in every image. In our study, the only difference in nerve angle was at the elbow, where a difference of less than 3° was observed for the ULNT1-DIST compared to P0 and ULNT1-STD. Despite this, no correlation was found between SWV and nerve angle. Therefore, nerve angle does not seem to significantly influence SWV measurements in this study.

Several limitations should be addressed.

First, the final ROM was measured only for the last joint of the sequence, such that other joints might move through different ranges. However, since participants had no joint limitations and similar ROM at the end of the ULNT1, any resultant variation in the mechanical forces acting on the nerve is likely to be minor.

The starting position adopted in our study may not implicate a complete and homogeneous unload of the MN, therefore, it cannot be fully discriminated if the amount of baseline difference in SWV between the two MN locations is due to regional variation in nerve characteristics (Rugel et al., 2020; Greening and Dilley, 2017; Andrade et al., 2022) or to a slightly different tension between the two MN segments. Along with this, the external forces acting on the nerve proceeding from surrounding tissues cannot be separated from tension in any position. For instance, movements that directly affect the length of the muscles surrounding the MN may contribute to a lateral transmission of force that can further affect nerve length and, consequently, local stiffness. These factors may impact nerve SWV measurements and influence the interpretation of our results.

5. Conclusions

MN SWV was influenced by the order of joint movements during neurodynamic testing. The ULNT1-STD and ULNT1-DIST showed a greater increase in MN SWV at the wrist compared to the ULNT1-PROX, whereas all sequences resulted in a similar MN SWV increase at the elbow. This suggests that a specific nerve segment may be subjected to different loading patterns based on joint movement order. However, these results must be interpreted with caution. as it was not possible to determine the exact amount of baseline neural load or the effect of surrounding tissues on MN SWV at each position. Additionally, these findings may not be generalized to other nerve locations or to pathological conditions, for which further research is needed.

CRediT authorship contribution statement

Gianluca Ciuffreda: Writing – original draft, Methodology, Data curation, Conceptualization. **Elena Estébanez-de-Miguel:** Writing – review & editing, Supervision, Formal analysis, Conceptualization. **Isabel Albarova-Corral:** Investigation, Data curation. **Miguel Malo-Urriés:** Investigation, Data curation. **Michael Shacklock:** Writing – review & editing, Conceptualization. **Alberto Montaner-Cuello:**

Writing – original draft, Data curation. **Elena Bueno-Gracia:** Writing – review & editing, Supervision, Methodology, Conceptualization.

References

Andrade, R.J., Nordez, A., Hug, F., et al., 2016. Non-invasive assessment of sciatic nerve stiffness during human ankle motion using ultrasound shear wave elastography. J. Biomech. 49 (3), 326–331. https://doi.org/10.1016/j.jbiomech.2015.12.017.

Andrade, R.J., Freitas, S.R., Hug, F., Coppieters, M.W., Sierra-Silvestre, E., Nordez, A., 2022. Spatial variation in mechanical properties along the sciatic and tibial nerves: an ultrasound shear wave elastography study. J. Biomech. 136. https://doi.org/10.1016/j.jbiomech.2022.111075.

Apelby-Albrecht, M., Andersson, L., Kleiva, I.W., Kvåle, K., Skillgate, E., Josephson, A., 2013. Concordance of upper limb neurodynamic tests with medical examination and magnetic resonance imaging in patients with cervical radiculopathy: a diagnostic cohort study. J. Manip. Physiol. Ther. 36 (9), 626–632. https://doi.org/10.1016/j.jmpt.2013.07.007.

Bercoff, J., Tanter, M., Fink, M., 2004. Supersonic shear imaging: a new technique for soft tissue elasticity mapping. IEEE Trans. Ultrason. Ferroelectrics Freq. Control 51 (4).

Boyd, B.S., Topp, K.S., Coppieters, M.W., 2013. Impact of movement sequencing on sciatic and tibial nerve strain and excursion during the straight leg raise test in embalmed cadavers. J. Orthop. Sports Phys. Ther. 43 (6), 398–403. https://doi.org/10.2519/jospt.2013.4413.

Brum, J., Bernal, M., Gennisson, J.L., Tanter, M., 2014. In vivo evaluation of the elastic anisotropy of the human Achilles tendon using shear wave dispersion analysis. Phys. Med. Biol. 59 (3), 505–523. https://doi.org/10.1088/0031-9155/59/3/505.

Bueno-Gracia, E., Tricás-Moreno, J.M., Fanlo-Mazas, P., et al., 2016. Validity of the upper limb neurodynamic test 1 for the diagnosis of carpal tunnel syndrome. The role of structural differentiation. Man. Ther. 22, 190–195. https://doi.org/10.1016/j.math.2015.12.007.

Bueno-Gracia, E., Pérez-Bellmunt, A., Estébanez-de-Miguel, E., et al., 2019. Differential movement of the sciatic nerve and hamstrings during the straight leg raise with ankle dorsiflexion: implications for diagnosis of neural aspect to hamstring disorders. Musculoskelet Sci Pract 43, 91–95. https://doi.org/10.1016/j.msksp.2019.07.011.

Bueno-Gracia, E., Pérez-Bellmunt, A., Estébanez-de-Miguel, E., et al., 2020a. Effect of cervical contralateral lateral flexion on displacement and strain in the median nerve and flexor digitorum superficialis at the wrist during the ULNT1 – cadaveric study. Musculoskelet Sci Pract 50. https://doi.org/10.1016/j.msksp.2020.102244.

Bueno-Gracia, E., Estébanez-de-Miguel, E., López-de-Celis, C., et al., 2020b. Effect of ankle dorsiflexion on displacement and strain in the tibial nerve and biceps femoris muscle at the posterior knee during the straight leg raise: investigation of specificity of nerve movement. Clin. BioMech. 75. https://doi.org/10.1016/j.clinbiomech.2020.105003.

Bueno-Gracia, E., González-Rueda, V., Pérez-Bellmunt, A., et al., 2021. Differential movement of the median nerve and biceps brachii at the elbow in human cadavers. Clin. BioMech. https://doi.org/10.1016/j.clinbiomech.2021.105370.

Bueno-Gracia, E., Fanlo-Mazas, P., Malo-Urriés, M., et al., 2024. Diagnostic accuracy of the upper limb neurodynamic test 1 using neurodynamic sequencing in diagnosis of carpal tunnel syndrome. Musculoskelet Sci Pract 69. https://doi.org/10.1016/j.msksp.2023.102897.

Butler, D., 1991. Mobilisation of the Nervous System, first ed. Churchill Livingstone, Edinburgh.

Carter, T.I., Pansy, B., Wolff, A.L., et al., 2009. Accuracy and reliability of three different techniques for manual goniometry for wrist motion: a cadaveric study. J. Hand Surg. 34 (8), 1422–1428. https://doi.org/10.1016/j.jhsa.2009.06.002.

Ciuffreda, G., Bueno-Gracia, E., Albarova-Corral, I., et al., 2024. In vivo effects of joint movement on nerve mechanical properties assessed with shear-wave elastography: a systematic review and meta-analysis. Diagnostics 14 (3). https://doi.org/10.3390/diagnostics14030343.

Coppieters, M.W., De Velde, M Van, Stappaerts, K.H., 2002a. Positioning in Anesthesiology, vol. 97. www.anesthesiology.org.

Coppieters, M., Stappaerts, K., Janssens, K., 2002b. Reliability of Detecting "Onset of Pain" and "Submaximal Pain" during Neural Provocation Testing of the Upper Quadrant, vol. 7.

Cuschieri, S., 2019. The STROBE guidelines. Saudi J. Anaesth. 13 (5), S31–S34. https://doi.org/10.4103/sja.SJA_543_18.

Elvey, R.L., 1997. Physical evaluation of the peripheral nervous system in disorders of pain and dysfunction. J. Hand Ther. 10 (2), 122–129. https://doi.org/10.1016/S0894-1130(97)80066-X.

Faul, F., Erdfelder, E., Lang, A.G., Buchner, A., 2007. G*Power 3: a flexible statistical power analysis program for the social, behavioral, and biomedical sciences. Behaviour Research Methods 39 (2), 175–191.

Greening, J., Dilley, A., 2017. Posture-induced changes in peripheral nerve stiffness measured by ultrasound shear-wave elastography. Muscle Nerve 55 (2), 213–222. https://doi.org/10.1002/mus.25245.

Hall, T.M., Elvey, R.L., 1999. Nerve trunk pain: physical diagnosis and treatment. Man. Ther. 4 (2), 63–73.

Herrington, L., Bendix, K., Cornwell, C., Fielden, N., Hankey, K., 2008. What is the normal response to structural differentiation within the slump and straight leg raise tests? Man. Ther. 13 (4), 289–294. https://doi.org/10.1016/j.math.2007.01.013.

Koo, T.K., Li, M.Y., 2016. A guideline of selecting and reporting intraclass correlation coefficients for reliability research. J Chiropr Med 15 (2), 155–163. https://doi.org/10.1016/j.jcm.2016.02.012.

LaStayo, P.C., Wheeler Donna, L., 1995. Reliability of passive wrist flexion and extension goniometric measurements: a multicenter study. Phys. Ther. 74 (2), 162–174.

Lee, S.H., Chang, J.M., Cho, N., et al., 2013. Practice guideline for the performance of breast ultrasound elastography. Ultrasonography 33 (1), 3–10. https://doi.org/10.14366/usg.13012.

Lee, S., Kwak, J., Lee, S., Cho, H., Oh, E., Park, J.W., 2019. Quantitative stiffness of the median nerve, flexor tendons, and flexor retinaculum in the carpal tunnel measured with acoustic radiation force impulse elastography in various wrist and finger positions. Medicine 98 (36). https://doi.org/10.1097/MD.0000000000017066.

Legakis, A., Boyd, B.S., 2012. The influence of scapular depression on upper limb neurodynamic test responses. J. Man. Manip. Ther. 20 (2), 75–82. https://doi.org/10.1179/2042618611Y.0000000020.

Lin, C.P., Chen, I.J., Chang, K.V., Wu, W.T., Özçakar, L., 2019. Utility of ultrasound elastography in evaluation of carpal tunnel syndrome: a systematic review and meta-analysis. Ultrasound Med. Biol. 45 (11), 2855–2865. https://doi.org/10.1016/j.ultrasmedbio.2019.07.409.

Lin, M., Chen, Y., Deng, W., et al., 2022. Quantifying the elasticity properties of the median nerve during the upper limb neurodynamic test 1. Appl. Bionics Biomech. 2022. https://doi.org/10.1155/2022/3300835.

Lohkamp, M., Small, K., 2011. Normal response to upper limb neurodynamic test 1 and 2A. Man. Ther. 16 (2), 125–130. https://doi.org/10.1016/j.math.2010.07.008.

Martínez, M.D.A., Cubas, C.L., Girbés, E.L., 2014. Ulnar nerve neurodynamic test: study of the normal sensory response in asymptomatic individuals. J. Orthop. Sports Phys. Ther. 44 (6), 450–456. https://doi.org/10.2519/jospt.2014.5207.

Mo, J., Xu, H., Qiang, B., et al., 2016. Bias of shear wave elasticity measurements in thin layer samples and a simple correction strategy. SpringerPlus 5 (1). https://doi.org/10.1186/s40064-016-2937-3.

Moran, R., Royuela, A., de Vargas, A.P., Lopez, A., Cepeda, Y., Martinelli, G., 2020. Carpal tunnel syndrome: diagnostic usefulness of ultrasound measurement of the median nerve area and quantitative elastographic measurement of the median nerve stiffness. J. Ultrasound Med. 39 (2), 331–339. https://doi.org/10.1002/jum.15111.

Nee, R.J., Yang, C.H., Liang, C.C., Tseng, G.F., Coppieters, M.W., 2010. Impact of order of movement on nerve strain and longitudinal excursion:A biomechanical study with implications for neurodynamic test sequencing. Man. Ther. 15 (4), 376–381. https://doi.org/10.1016/j.math.2010.03.001.

Nee, R.J., Jull, G.A., Vicenzino, B., Coppieters, M.W., 2012. The validity of upper-limb neurodynamic tests for detecting peripheral neuropathic pain. J. Orthop. Sports Phys. Ther. 42 (5), 413–424. https://doi.org/10.2519/jospt.2012.3988.

Nightingale, K., 2011. Acoustic radiation force impulse (arfi) imaging: a review. Curr. Med. Imag. Rev. 7 (4), 328–339. https://doi.org/10.2174/157340511798038657.

Noah Weiss, B.D., Leonard, Gordon Md, Bloom, T., Rempel, D.M., Francisco, California S., 1995. Position of the Wrist Associated with the Lowest Carpal-Tunnel Pressure: Implications for Splint Design, vol. 77.

Oliver, G.S., Rushton, A., 2011. A study to explore the reliability and precision of intra and inter-rater measures of ULNT1 on an asymptomatic population. Man. Ther. 16 (2), 203–206. https://doi.org/10.1016/j.math.2010.05.009.

Pesonen, J., Shacklock, M., Suomalainen, J.S., et al., 2021. Extending the straight leg raise test for improved clinical evaluation of sciatica: validity and diagnostic performance with reference to the magnetic resonance imaging. BMC Muscoskel. Disord. 22 (1). https://doi.org/10.1186/s12891-021-04649-z.

Riddle DL, Rothstein JM, Lamb RL. Goniometric Reliability in a Clinical Setting Shoulder Measurements PHYSICAL THERAPY.

Riley, S.P., Grimes, J.K., Calandra, K., Foster, K., Peet, M., Walsh, M.T., 2020. Agreement and reliability of median neurodynamic test 1 and resting scapular position. J Chiropr Med 19 (4), 203–212. https://doi.org/10.1016/j.jcm.2020.09.002.

Rothstein, J.M., Miller, P.J., Roettger, R.F., 1983. Goniometric Reliability in a Clinical Setting Elbow and Knee Measurements, vol. 63.

Rugel, C.L., Franz, C.K., Lee, S.S.M., 2020. Influence of limb position on assessment of nerve mechanical properties by using shear wave ultrasound elastography. Muscle Nerve 61 (5), 616–622. https://doi.org/10.1002/mus.26842.

Schmid, A.B., Brunner, F., Luomajoki, H., et al., 2009. Reliability of clinical tests to evaluate nerve function and mechanosensitivity of the upper limb peripheral nervous system. BMC Muscoskel. Disord. 10. https://doi.org/10.1186/1471-2474-10-11.

Shacklock, M., 1989. The Plantarflexion/Inversion Straight Leg Raise: A Normative Study and Investigation into the Effect of Passive Cervical Flexion and Altering Order of Component Movements on the Symptom Response [thesis].

Shacklock, M., 2005a. Improving application of neurodynamic (neural tension) testing and treatments: a message to researchers and clinicians. Man. Ther. 10 (3), 175–179. https://doi.org/10.1016/j.math.2005.03.001.

Shacklock, M., 2005b. Clinical Neurodynamics. Elsevier, Oxford.

Shiina, T., Nightingale, K.R., Palmeri, M.L., et al., 2015. WFUMB guidelines and recommendations for clinical use of ultrasound elastography: Part 1: basic principles and terminology. Ultrasound Med. Biol. 41 (5), 1126–1147. https://doi.org/10.1016/j.ultrasmedbio.2015.03.009.

Talebi, G.A., Oskouei, A.E., Shakori, S.K., 2012. Reliability of upper limb tension test 1 in normal subjects and patients with carpal tunnel syndrome. J. Back Musculoskelet. Rehabil. 25 (3), 209–214. https://doi.org/10.3233/BMR-2012-0330.

Taljanovic, M.S., Gimber, L.H., Becker, G.W., et al., 2017. Shear-wave elastography: basic physics and musculoskeletal applications. Radiographics 37 (3), 855–870. https://doi.org/10.1148/rg.2017160116.

Trillos, M.C., Soto, F., Briceno-Ayala, L., 2018. Upper limb neurodynamic test 1 in patients with clinical diagnosis of carpal tunnel syndrome: a diagnostic accuracy study. J. Hand Ther. 31 (3), 333–338. https://doi.org/10.1016/j.jht.2017.05.004.

Tsai, Y.Y., 1995. Tension Change in the Ulnar Nerve by Different Order of Upper Limb Tension Test [thesis].

Vanti, C., Conteddu, L., Guccione, A., et al., 2010. The upper limb neurodynamic test 1: intra- and intertester reliability and the effect of several repetitions on pain and resistance. J. Manip. Physiol. Ther. 33 (4), 292–299. https://doi.org/10.1016/j.jmpt.2010.03.003.

Vanti, C., Bonfiglioli, R., Calabrese, M., et al., 2011. Upper limb neurodynamic test 1 and symptoms reproduction in carpal tunnel syndrome. A validity study. Man. Ther. 16 (3), 258–263. https://doi.org/10.1016/j.math.2010.11.003.

Vanti, C., Bonfiglioli, R., Calabrese, M., Marinelli, F., Violante, F.S., Pillastrini, P., 2012. Relationship between interpretation and accuracy of the upper limb neurodynamic test 1 in carpal tunnel syndrome. J. Manip. Physiol. Ther. 35 (1), 54–63. https://doi.org/10.1016/j.jmpt.2011.09.008.

Wainner, R., Fritz, J.M., Irrgang, J.J., Boninger, M.L., Delitto, A., Stephen Allison, C., 2003. Reliability and diagnostic accuracy of the clinical examination and patient self-report measures for cervical radiculopathy. Spine 28 (1), 52–62.

Wainner, R.S., Fritz, J.M., Irrgang, J.J., Delitto, A., Allison, S., Boninger, M.L., 2005. Development of a clinical prediction rule for the diagnosis of carpal tunnel syndrome. Arch. Phys. Med. Rehabil. 86 (4), 609–618. https://doi.org/10.1016/j.apmr.2004.11.008.

Wee, T.C., Simon, N.G., 2019. Ultrasound elastography for the evaluation of peripheral nerves: a systematic review. Muscle Nerve 60 (5), 501–512. https://doi.org/10.1002/mus.26624.

World Medical Association declaration of Helsinki, 2013. Ethical principles for medical research involving human subjects. JAMA, J. Am. Med. Assoc. 310 (20), 2191–2194. https://doi.org/10.1001/jama.2013.281053.

Yoon, J.H., Lee, J.M., Joo, I., et al., 2014. Hepatic fibrosis: prospective comparison of MR elastography and us shear-wave elastography for evaluation. Radiology 273 (3), 772–781. https://doi.org/10.1148/radiol.14132000.

Youk, J.H., Son, E.J., Park, A.Y., Kim, J.A., 2013. Shear-wave elastography for breast masses: local shear wave speed (m/s) versus Young modulus (kPa). Ultrasonography 33 (1), 34–39. https://doi.org/10.14366/usg.13005.

Zakrzewski, J., Zakrzewska, K., Pluta, K., Nowak, O., Miłoszewska-Paluch, A., 2019. Ultrasound elastography in the evaluation of peripheral neuropathies: a systematic review of the literature. Pol. J. Radiol. 84, 581–591. https://doi.org/10.5114/pjr.2019.91439.